G^0 Pythagorean-Hodograph Curves Closest to Prescribed Planar Bézier Curves

Wenqing FEI,   Yongxia HAO*

School of Mathematical Sciences, Jiangsu University, Jiangsu 212000, *P. R. China*

Abstract The task of identifying the quintic PH curve G^0 "closest" to a given planar Bézier curve with or without prescribed arc length is discussed here using Gauss-Legendre polygon and Gauss-Lobatto polygon respectively. By expressing the sum of squared differences between the vertices of Gauss-Legendre or Gauss-Lobatto polygon of a given Bézier and those of a PH curve, it is shown that this problem can be formulated as a constrained polynomial optimization problem in certain real variables, subject to two or three quadratic constraints, which can be efficiently solved by Lagrange multiplier method and Newton-Raphson iteration. Several computed examples are used to illustrate implementations of the optimization methodology. The results demonstrate that compared with Bézier control polygon, the method with Gauss-Legendre and Gauss-Lobatto polygon can produce the G^0 PH curve closer to the given Bézier curve with close arc length. Moreover, good approximations with prescribed arc length can also be achieved.

Keywords Pythagorean-hodograph curves; Gauss-Legendre polygon; Gauss-Lobatto polygon; constrained optimization; Lagrange multiplier; Newton-Raphson iteration

MR(2020) Subject Classification 65D17; 65D18

1. Introduction

Pythagorean-hodograph (PH) curves, introduced by [1], are a special type of polynomial curves, which have the unique property that their parametric speed functions are also polynomials of the curve parameter. The PH property enables us to compute the arc length of the curve exactly without numerical integration. Another important advantage of PH curves is that their offset curves are rational curves, so we do not need to rely on approximation algorithms for offset computation. One may consult [2] for more details on PH curves from algebraic frameworks to practical applications.

Recently, the problem of identifying the planar PH curve that is "closest" to a given Bézier curve, and has the same end points (or end points and tangents), was considered in [3]. The "closeness" measure employed in the context is the root-mean-square magnitude of the differences between pairs of corresponding Bézier control points for the two curves. Using the complex representation for planar curves, it is shown that this problem can be reduced to the minimization of a quartic penalty function in certain real variables subject to two quadratic constraints.

The results highlight four noteworthy points: (1) the G^0 case conforms more closely than G^1 case, since it incorporates more free optimization parameters; (2) the closest PH quintic curves offer better approximations to convex cubic segments than to inflectional segments; (3) closest approximations of quintic Bézier curves by PH quintics can be achieved for curves without several curvature variation; (4) invoking the Lagrange multiplier method, the problem can be efficiently solved to machine precision by a few Newton-Raphson iterations.

Noted that a PH curve has fewer degrees of freedom than a Bézier curve of the same degree has, since the Bézier control points of a PH curve should satisfy certain algebraic constraints. In fact, the identification of PH curves from the Bézier polygons is not a trivial task. Recently, Farouki et al. [4] suggested the method to determine whether a given Bézier curve is in fact a PH curve, and to compute the parameters of the PH curve. They also presented the method of local modification of quintic PH spline curve while maintaining the PH property [5]. This situation suggests that a Bézier control polygon is not appropriate to control a PH curve. As an alternative to the Bézier polygon, the Gauss-Legendre polygon was recently introduced in [6, 7] as the representative of PH curves. The Gauss-Legendre polygon with enough number of edges has the same degrees of freedom as the PH curve, interpolates the end points and has the same arc length as the PH curve. These properties make it a rectifying control polygon and a nice tool to control the shape of the PH curve. Moreover, the procedure to compute the PH curves from a given rectifying control polygon is developed based on the Bernstein-Vandermonde linear system. However, a crucial limitation of the Gauss-Legendre polygon is the lack of the end tangent representation, because all the nodes of the Gauss-Legendre quadrature are the interior ones. As a remedy to this problem, the Gauss-Lobatto polygon, which has the end tangent interpolation property by nature, was proposed in [8] as an alternative. Moreover, with adequate number of edges, it still interpolates the end points and has the same arc length as the PH curve.

Our goal in this paper is the development of a novel approach to constructing planar PH curves with or without prescribed arc length based on identifying, for a given planar Bézier curve, the "closest" PH curve of related degree based on Gauss-Lobatto polygon and Gauss-Legendre polygon respectively. As more end constraints are imposed, the number of free parameters available diminishes and consequently the "closeness" of the PH curve to the given Bézier curve will generally be reduced, we only discuss the G^0 "closeness" case in this context. The methodology presented herein employs a constrained optimization approach to determine the PH curve whose Gauss-Legendre or Gauss-Lobatto control points are as close as possible to those of a prescribed Bézier curve. The results demonstrate that compared with Bézier control polygon, our method can produce the G^0 PH curve closer to the given Bézier curve with close arc length for convex and inflectional curves. Moreover, good approximations with specified arc length can also be achieved.

The plan for the remainder of this paper is as follows. Section 2 briefly reviews the fundamental properties of PH curves, the Gauss-Legendre polygon and Gauss-Lobatto polygon. Identification of the quintic PH curve (with specified arc length) that is closest to a given planar Bézier curve is then formulated as a constrained optimization problem in Section 3, using the

Gauss-Legendre and Gauss-Lobatto polygon respectively. Section 4 then illustrates an implementation of the method through some representative computed examples. Finally, Section 5 concludes the main contributions of this study.

2. Preliminary

In this section, we review some basic knowledges about PH curves and the two types of polygons, namely the Gauss-Legendre polygon and Gauss-Lobatto polygon.

2.1. Planar Pythagorean-hodograph curves

For the simplicity of the representation, we use the complex notation for planar curves. A point $z = (x, y)$ in $\mathbb{R}^2$ is identified with the complex number $z = x + iy$ in $\mathbb{C}$. Similarly, a planar parametric curve $\mathbf{r}(t) = (x(t), y(t))$ can be identified with a complex valued function $\mathbf{r}(t) = x(t) + iy(t)$.

A planar polynomial curve $\mathbf{r}(t) = x(t) + iy(t)$ is called a PH curve if and only if there exist real polynomials $u(t)$ and $v(t)$ which satisfy

$$x'(t) = u^2(t) - v^2(t), \quad y'(t) = 2u(t)v(t).$$

This structure is embodied in the complex representation [9], wherein a PH curve $\mathbf{r}$ of degree $n = 2m + 1$ is generated from a degree m complex polynomial

$$\mathbf{w}(t) = u(t) + iv(t) = \sum_{k=0}^{m} \mathbf{w}_k \binom{m}{k} (1-t)^{m-k} t^k \tag{2.1}$$

by integration of the expression $\mathbf{r}' = \mathbf{w}^2$.

2.2. Gauss-Legendre polygon

The concept of Gauss-Legendre polygon for PH curves was proposed in [6] based on the Gauss-Legendre quadrature. The key property of the Gauss-Legendre quadrature

$$I_m = \sum_{k=0}^{m-1} \omega_{m,k} f(\tau_{m,k})$$

with m nodes of a polynomial function f on $[-1, 1]$ is that it gives the exact integral if the degree of f is less than or equal to $2m - 1$. Table 1 lists the nodes $\tau_{m,k}$ and weights $\omega_{m,k}$ up to order 5. The following theorem presents the error of Gauss-Legendre quadrature with m nodes for a polynomial function f defined on $[0, 1]$ (see [11, 13]).

Theorem 2.1 ([13])   *Let $f(x) \in C^{2m}[0, 1]$. Then*

$$\int_0^1 f(t) \mathrm{d}t = \sum_{k=0}^{m-1} \frac{\omega_{m,k}}{2} f(\frac{1 + \tau_{m,k}}{2}) + E_m(f),$$

where

$$E_m(f) = \frac{[(m)!]^4}{(2m+1)[(2m)!]^3} f^{(2m)}(\xi), \quad \xi \in [0, 1].$$

Number of nodes (m)	Nodes $(\tau_{m,k})$	Weights $(\omega_{m,k})$
1	0	2
2	$\pm\sqrt{\frac{1}{3}}$	1
3	$0, \pm\sqrt{\frac{3}{5}}$	$\frac{8}{9}, \frac{5}{9}$
4	$\pm\sqrt{\frac{3}{7}-\frac{2}{7}\sqrt{\frac{6}{5}}}, \pm\sqrt{\frac{3}{7}+\frac{2}{7}\sqrt{\frac{6}{5}}}$	$\frac{18+\sqrt{30}}{36}, \frac{18-\sqrt{30}}{36}$
5	$0, \pm\frac{1}{3}\sqrt{5-2\sqrt{\frac{10}{7}}}, \pm\frac{1}{3}\sqrt{5+2\sqrt{\frac{10}{7}}}$	$\frac{128}{225}, \frac{332+13\sqrt{70}}{900}, \frac{332-13\sqrt{70}}{900}$

Table 1 Nodes and weights of Gauss-Legendre quadrature up to order 5

Definition 2.2 *Let* $\mathbf{p}$ *be a regular curve in* $\mathbb{R}^q$ *defined on* $[0,1]$*. The Gauss-Legendre polygon of* $\mathbf{p}$ *with* m *edges is defined by*

$$G_m(\mathbf{p}) = [\mathbf{p}_0 \cdots \mathbf{p}_m],$$

where

$$\mathbf{p}_0 = \mathbf{p}(0),$$
$$\mathbf{p}_{k+1} = \mathbf{p}_k + \frac{\omega_{m,k}}{2}\mathbf{p}'(\frac{1+\tau_{m,k}}{2}), \quad k = 0, 1, \ldots, m-1.$$

It can be easily proved from the definition that the Gauss-Legendre polygon with adequate number of edges for a polynomial curve has the end point interpolation property, as demonstrated in the following theorem.

Theorem 2.3 *Let* $\mathbf{p}$ *be a polynomial curve of degree* l *in* $\mathbb{R}^q$ *defined on* $[0,1]$*. If* $m \geq \frac{l}{2}$*, then the Gauss-Legendre polygon* $G_m(\mathbf{p})$ *has the end point interpolation property: that is,* $\mathbf{p}_m = \mathbf{p}(1)$*.*

The arc-length formula of a differentiable curve is motivated by the piecewise linear approximation. For a regular curve $\mathbf{p}$ defined on $[0,1]$, if we choose a partition $0 = t_0 < t_1 < \cdots < t_{n+1} = 1$ of $[0,1]$, then the polygon connecting the sequence of points $\mathbf{p}(t_0), \mathbf{p}(t_1), \ldots, \mathbf{p}(t_{n+1})$ approximates the given curve $\mathbf{p}$. The length of this polygon converges to the arc length of $\mathbf{p}$ as the partition size tends to 0. For a PH curve $\mathbf{p}$, by Theorem 2.1, the length of its Gauss-Legendre polygon with adequate edge is the same as the arc length of $\mathbf{p}$, while for a polynomial curve, the length of its Gauss-Legendre polygon can be regarded as the approximation of its arc length.

Theorem 2.4 ([6]) *Let* $\mathbf{r}$ *be a PH curve of degree* $2n+1$ *defined on* $[0,1]$*. Then its Gauss-Legendre polygon* $[\mathbf{p}_0\mathbf{p}_1 \cdots \mathbf{p}_m]$ *with* $m \geq n+1$ *is a rectifying polygon of* $\mathbf{r}$*, which means the length of the polygon is the same as the arc length of* $\mathbf{r}$*.*

Theorem 2.5 ([6]) *For a given polygon* $[\mathbf{p}_0\mathbf{p}_1 \cdots \mathbf{p}_{n+1}]$ *of* $n+1$ *segments, there exist* 2^n *PH curves of degree* $2n+1$ *whose rectifying polygon is* $[\mathbf{p}_0\mathbf{p}_1 \cdots \mathbf{p}_{n+1}]$*.*

2.3. Gauss-Lobatto polygon

Although the Gauss-Legendre polygon is a nice representative of PH curves, a clear drawback of it is that it does not determine the end tangent vectors. This is because all the nodes

of the Gauss-Legendre quadrature are the interior ones. So, the Gauss-Lobatto polygon was introduced in [8] based on the Gauss-Lobatto quadrature, which utilizes both end parameters $0, 1$ as preselected nodes.

For an integrable function f on $[0, 1]$, the Gauss-Lobatto quadrature is

$$\bar{I}(f; [0, 1]) = \frac{\bar{\omega}_{m,0}}{2} f(0) + \frac{\bar{\omega}_{m,m-1}}{2} f(1) + \sum_{k=1}^{m-2} \frac{\bar{\omega}_{m,k}}{2} f(\frac{1 + \bar{\tau}_{m,k}}{2}).$$

Table 2 lists the values of the nodes $\bar{\tau}_{m,k}$ and the weights $\bar{\omega}_{m,k}$ for small number of nodes. The following theorem shows the complete formula of Gauss-Lobatto integration rule [10, 12].

Theorem 2.6 ([12]) *Let* $f(x) \in C^{2m-2}[0, 1]$. *Then we have*

$$\int_0^1 f(t) \mathrm{d}t = \sum_{k=0}^{m-1} \frac{\bar{\omega}_{m,k}}{2} f(\frac{1 + \bar{\tau}_{m,k}}{2}) + E_m(f),$$

where

$$E_m(f) = \frac{-m(m-1)^3[(m-2)!]^4}{(2m-1)[(2m-2)!]^4} f^{(2m-2)}(\xi), \quad \xi \in [0, 1].$$

Based on Theorem 2.6, the Gauss-Lobatto quadrature $\bar{I}_m$ with m nodes evaluates the exact integral of polynomial of degree up to $2m-3$ and the Gauss-Lobatto polygon with adequate edges acquires the rectifying property if the given curve $\mathbf{p}$ is a PH curve. Moreover, it demonstrates that the length of the Gauss-Lobatto polygon for a polynomial curve can also be regarded as the approximation of its arc length.

Number of nodes m	Nodes $(\bar{\tau}_{m,k})$	Weights $(\bar{\omega}_{m,k})$
2	± 1	1
3	$\pm 1, 0$	$\frac{1}{3}, \frac{4}{3}$
4	$\pm 1, \pm\sqrt{\frac{1}{5}}$	$\frac{1}{6}, \frac{5}{6}$
5	$\pm 1, \pm\sqrt{\frac{3}{7}}, 0$	$\frac{1}{10}, \frac{49}{90}, \frac{32}{45}$
6	$\pm 1, \pm\sqrt{\frac{1}{3} + \frac{2\sqrt{7}}{21}}, \pm\sqrt{\frac{1}{3} - \frac{2\sqrt{7}}{21}}$	$\frac{1}{15}, \frac{14-\sqrt{7}}{30}, \frac{14+\sqrt{7}}{30}$
7	$\pm 1, \pm\sqrt{\frac{5}{11} + \frac{2}{11}\sqrt{\frac{5}{3}}}, \pm\sqrt{\frac{5}{11} - \frac{2}{11}\sqrt{\frac{5}{3}}}, 0$	$\frac{1}{21}, \frac{124-7\sqrt{15}}{350}, \frac{124+7\sqrt{15}}{350}, \frac{256}{525}$

Table 2 Nodes and weights of Gauss-Lobatto quadrature up to order 5

Definition 2.7 ([8]) *Let* $\mathbf{p}$ *be a regular curve in* $\mathbb{R}^q$ *defined on* $[0, 1]$. *The Gauss-Lobatto polygon of* $\mathbf{p}$ *with* m *edges is defined by*

$$\bar{G}_m(\mathbf{p}) = [\mathbf{p}_0 \mathbf{p}_1 \cdots \mathbf{p}_m],$$

where

$$\mathbf{p}_0 = \mathbf{p}(0),$$
$$\mathbf{p}_{k+1} = \mathbf{p}_k + \frac{\bar{\omega}_{m,k}}{2} \mathbf{p}'(\frac{1 + \bar{\tau}_{m,k}}{2}), \quad k = 0, 1, \ldots, m-1.$$

If **p** is a polynomial curve, then its Gauss-Lobatto polygon with adequate number of edges has the end point interpolation property and rectifying property.

Theorem 2.8 ([8]) *Let **p** be a polynomial curve of degree l in $\mathbb{R}^q$ defined on $[0, 1]$. If $m \geq \frac{l}{2} + 1$, then the Gauss-Lobatto polygon $\bar{G}_m(\mathbf{p})$ has the end point interpolation property: that is, $\mathbf{p}_m = \mathbf{p}(1)$.*

Theorem 2.9 ([8]) *Let **p** be a PH curve of degree $2n + 1$ in either $\mathbb{R}^2$ or $\mathbb{R}^3$ defined on $[0, 1]$. If $m \geq n + 2$, then the Gauss-Lobatto polygon $\bar{G}_m(\mathbf{p})$ is a rectifying polygon.*

3. Constrained optimization problem

Based on Gauss-Legendre and Gauss-Lobatto polygon, the task of identifying the planar PH curve **p** "closest" to a prescribed Bézier curve **q** is discussed in this section. As shown in [3], the more end constraints imposed, the less close of the PH curve to the given Bézier curve, therefore, we only discuss the G^0 quintic PH curves "closest" to prescribed planar Bézier curves. The measure of "closeness" is based on the sum of squared distances between corresponding vertices of the Gauss-Legendre or Gauss-Lobatto polygon of the two curves. The objective function and constraints may be expressed in terms of the coefficients of the preimage polynomial (2.1) of **p** and constants determined by the control points of **q**.

To facilitate the analysis, it is convenient to use canonical form, whose initial and final points coincide with the values 0 and 1 on the real axis. A plane curve can be mapped to canonical form by a translation/rotation/scaling transformation, and can be mapped back to its original position by the inverse of that transformation.

Consider a planar cubic Bézier curve **q** given in canonical form

$$\mathbf{q}(t) = \sum_{k=0}^{3} \mathbf{c}_k \binom{3}{k} (1-t)^{3-k} t^k \tag{3.1}$$

with $\mathbf{c}_0 = 0$ and $\mathbf{c}_3 = 1$. We want to identify the quintic PH curve **p** "closest" to **q** that has the same end points. **p** may be generated by substituting a quadratic complex polynomial

$$\mathbf{w}(t) = \mathbf{w}_0 (1-t)^2 + 2\mathbf{w}_1 (1-t)t + \mathbf{w}_2 t^2$$

into $\mathbf{p}' = \mathbf{w}^2$ and integrating. The control points of the Bézier representation

$$\mathbf{p}(t) = \sum_{k=0}^{5} \mathbf{b}_k \binom{5}{k} (1-t)^{5-k} t^k$$

are then determined [3] from the coefficients $\mathbf{w}_0, \mathbf{w}_1, \mathbf{w}_2$ as

$$\mathbf{b}_1 = \mathbf{b}_0 + \frac{1}{5}\mathbf{w}_0^2, \quad \mathbf{b}_2 = \mathbf{b}_1 + \frac{1}{5}\mathbf{w}_0\mathbf{w}_1, \quad \mathbf{b}_3 = \mathbf{b}_2 + \frac{2\mathbf{w}_1^2 + \mathbf{w}_0\mathbf{w}_2}{15},$$

$$\mathbf{b}_4 = \mathbf{b}_3 + \frac{1}{5}\mathbf{w}_1\mathbf{w}_2, \quad \mathbf{b}_5 = \mathbf{b}_4 + \frac{1}{5}\mathbf{w}_2^2 \tag{3.2}$$

with $\mathbf{b}_0 = \mathbf{c}_0 = 0$. The end point interpolation $\mathbf{p}(1) = \mathbf{q}(1)$ yields the following constraints [3]

$$2\mathbf{w}_1^2 + 3(\mathbf{w}_0 + \mathbf{w}_2)\mathbf{w}_1 + 3(\mathbf{w}_0^2 + \mathbf{w}_2^2) + \mathbf{w}_0\mathbf{w}_2 - 15 = 0. \tag{3.3}$$

In the following, discussion of identifying the G^0 PH quintic curve $\mathbf{p}$ "closest" to a given Bézier curve $\mathbf{q}$ (with prescribed arc length) is treated.

3.1. G^0 PH quintic closest to a cubic Bézier curve by Gauss-Legendre polygon

In this section, we identify the PH quintic curve $\mathbf{p}$ "closest" to a given planar cubic Bézier curve $\mathbf{q}$ by minimizing the squared distance between their vertices of Gauss-Legendre polygons. By Theorem 2.3, in order to make sure that the Gauss-Legendre polygons of $\mathbf{p}$ and $\mathbf{q}$ both have the end interpolation property, their edge number m must satisfy $m \geq 3$. Hence we discuss $m = 3, 4, 5$ respectively.

When $m = 3$, by Definition 2.2, the vertices of the Gauss-Legendre polygons of cubic Bézier curve $\mathbf{q}$ and quintic PH curve $\mathbf{p}$ are

$$\mathbf{q}_0 = 0, \quad \mathbf{q}_1 = \frac{(\sqrt{15}+2)\mathbf{c}_1 + (\sqrt{15}-2)\mathbf{c}_2}{12} + \frac{4 - \sqrt{15}}{12},$$
$$\mathbf{q}_2 = \frac{(\sqrt{15}-2)\mathbf{c}_1 + (\sqrt{15}+2)\mathbf{c}_2}{12} + \frac{8 - \sqrt{15}}{12}, \quad \mathbf{q}_3 = 1 \tag{3.4}$$

and

$$\begin{aligned}
\mathbf{p}_0 =&\, 0, \\
\mathbf{p}_1 =&\, \frac{1}{1080}[48\sqrt{15}\mathbf{w}_0^2 + (36\sqrt{15} - 45)\mathbf{w}_0\mathbf{w}_1 + (16\sqrt{15} - 50)\mathbf{w}_1^2 + \\
&\, (8\sqrt{15} - 25)\mathbf{w}_0\mathbf{w}_2 + (12\sqrt{15} - 45)\mathbf{w}_1\mathbf{w}_2 + (465 - 120\sqrt{15})], \\
\mathbf{p}_2 =&\, \frac{1}{1080}[48\sqrt{15}\mathbf{w}_0^2 + (36\sqrt{15} + 45)\mathbf{w}_0\mathbf{w}_1 + (16\sqrt{15} + 50)\mathbf{w}_1^2 + \\
&\, (8\sqrt{15} + 25)\mathbf{w}_0\mathbf{w}_2 + (12\sqrt{15} + 45)\mathbf{w}_1\mathbf{w}_2 + (615 - 120\sqrt{15})], \\
\mathbf{p}_3 =&\, 1, \tag{3.5}
\end{aligned}$$

respectively. We identify the quintic PH curve $\mathbf{p}$ by minimizing the quantity

$$\Delta = |\mathbf{p}_1 - \mathbf{q}_1|^2 + |\mathbf{p}_2 - \mathbf{q}_2|^2. \tag{3.6}$$

Substituting (3.4) and (3.5) into (3.6), simplifying, omitting terms that do not depend on $\mathbf{w}_0, \mathbf{w}_1, \mathbf{w}_2$, we obtain the following reduced form

$$\begin{aligned}
\Delta =&\, \frac{1}{108}[576\bar{\mathbf{w}}_0^2(12\mathbf{w}_0^2 + 9\mathbf{w}_0\mathbf{w}_1 + 4\mathbf{w}_1^2 + 2\mathbf{w}_0\mathbf{w}_2 + 3\mathbf{w}_1\mathbf{w}_2) + \\
&\, (2\bar{\mathbf{w}}_1^2 + \bar{\mathbf{w}}_0\bar{\mathbf{w}}_2)(1152\mathbf{w}_0^2 + 1089\mathbf{w}_0\mathbf{w}_1 + 634\mathbf{w}_1^2 + 317\mathbf{w}_0\mathbf{w}_2 + 513\mathbf{w}_1\mathbf{w}_2) + \\
&\, 9\bar{\mathbf{w}}_0\bar{\mathbf{w}}_1(576\mathbf{w}_0^2 + 477\mathbf{w}_0\mathbf{w}_1 + 242\mathbf{w}_1^2 + 121\mathbf{w}_0\mathbf{w}_2 + 189\mathbf{w}_1\mathbf{w}_2) + \\
&\, 27\bar{\mathbf{w}}_1\bar{\mathbf{w}}_2(64\mathbf{w}_0^2 + 63\mathbf{w}_0\mathbf{w}_1 + 38\mathbf{w}_1^2 + 19\mathbf{w}_0\mathbf{w}_2 + 31\mathbf{w}_1\mathbf{w}_2)] + \operatorname{Re}(T_1 - T_2 - T_3), \tag{3.7}
\end{aligned}$$

where

$$\begin{aligned}
T_1 =&\, \frac{1}{9}(31\sqrt{15} - 120)(12\mathbf{w}_0^2 + 4\mathbf{w}_1^2 + 9\mathbf{w}_0\mathbf{w}_1 + 2\mathbf{w}_0\mathbf{w}_2 + 3\mathbf{w}_1\mathbf{w}_2), \\
T_2 =&\, \bar{\mathbf{q}}_1[48\sqrt{15}\mathbf{w}_0^2 + (36\sqrt{15} - 45)\mathbf{w}_0\mathbf{w}_1 + (16\sqrt{15} - 50)\mathbf{w}_1^2 + (8\sqrt{15} - 25)\mathbf{w}_0\mathbf{w}_2 + \\
&\, (12\sqrt{15} - 45)\mathbf{w}_1\mathbf{w}_2],
\end{aligned}$$

$$T_3 = \bar{\mathbf{q}}_2[48\sqrt{15}\mathbf{w}_0^2 + (36\sqrt{15} + 45)\mathbf{w}_0\mathbf{w}_1 + (16\sqrt{15} + 50)\mathbf{w}_1^2 + (8\sqrt{15} + 25)\mathbf{w}_0\mathbf{w}_2 +$$
$$(12\sqrt{15} + 45)\mathbf{w}_1\mathbf{w}_2].$$

Writing $\mathbf{w}_k = u_k + iv_k$ for $k = 0, 1, 2$, the reduced objective function Δ can be expressed as $\Delta(u_0, v_0, u_1, v_1, u_2, v_2)$ that are subject to the real and imaginary parts of (3.3), which can be written as

$$g(u_0, v_0, u_1, v_1, u_2, v_2) = 0, \quad h(u_0, v_0, u_1, v_1, u_2, v_2) = 0, \tag{3.8}$$

where

$$g = 2(u_1^2 - v_1^2) + 3(u_0u_1 - v_0v_1) + 3(u_1u_2 - v_1v_2) +$$
$$3(u_0^2 - v_0^2) + 3(u_2^2 - v_2^2) + u_0u_2 - 15,$$
$$h = 4u_1v_1 + 3(u_0v_1 + u_1v_0) + 3(u_1v_2 + u_2v_1) + 6u_0v_0 +$$
$$6u_2v_2 + u_0v_2 + v_2u_0.$$

The goal is to minimize $\Delta(u_0, v_0, u_1, v_1, u_2, v_2)$ subject to the constraints (3.8). By Lagrange multiplier method, this can be achieved by solving the system of eight polynomial equations:

$$f_1 = \frac{\partial\Delta}{\partial u_0} + \alpha\frac{\partial g}{\partial u_0} + \beta\frac{\partial h}{\partial u_0} = 0, \quad f_2 = \frac{\partial\Delta}{\partial v_0} + \alpha\frac{\partial g}{\partial v_0} + \beta\frac{\partial h}{\partial v_0} = 0,$$
$$f_3 = \frac{\partial\Delta}{\partial u_1} + \alpha\frac{\partial g}{\partial u_1} + \beta\frac{\partial h}{\partial u_1} = 0, \quad f_4 = \frac{\partial\Delta}{\partial v_1} + \alpha\frac{\partial g}{\partial v_1} + \beta\frac{\partial h}{\partial v_1} = 0,$$
$$f_5 = \frac{\partial\Delta}{\partial u_2} + \alpha\frac{\partial g}{\partial u_2} + \beta\frac{\partial h}{\partial u_2} = 0, \quad f_6 = \frac{\partial\Delta}{\partial v_2} + \alpha\frac{\partial g}{\partial v_2} + \beta\frac{\partial h}{\partial v_2} = 0,$$
$$f_7 = g = 0, \quad f_8 = h = 0.$$

The Newton-Raphson iteration offers an accurate and efficient approach to solving this system of equations [3]. It is defined by the relations

$$\mathbf{x}_{k+1} = \mathbf{x}_k + \delta\mathbf{x}_k, \quad \mathbf{M}_k\delta\mathbf{x}_k = -\mathbf{f}_k,$$

where

$$\mathbf{x} = (u_0, v_0, u_1, v_1, u_2, v_2, \alpha, \beta)^{\mathrm{T}}$$

is the unknown vector, $\mathbf{M}$ is the corresponding 8×8 Jacobian matrix,

$$\mathbf{f} = (f_1, f_2, f_3, f_4, f_5, f_6, f_7, f_8)^{\mathrm{T}}$$

and the subscripts on $\mathbf{M}$ and $\mathbf{f}$ indicate that they are to be evaluated at $\mathbf{x}_k$. Note that the proposed approach for solving the constrained minimization problem should be regarded as a heuristic, whose success will depend on the starting point for the Newton method. Moreover, there is no guarantee that this approach will always find a global minimizer.

The cases of $m = 4, 5$ can be discussed similarly.

3.2. G^0 **PH quintic closest to a cubic Bézier curve by Gauss-Lobatto polygon**

In this section, we identify the PH quintic curve $\mathbf{p}$ "closest" to the cubic Bézier curve $\mathbf{q}$ by minimizing the squared distance between their vertices of the Gauss-Lobatto polygons. By

Theorem 2.8, in order to make sure that the Gauss-Lobatto polygons of $\mathbf{p}$ and $\mathbf{q}$ both have the end interpolation property, their edge number m must satisfy $m \geq 4$. Here we discuss $m = 4, 5, 6, 7$ respectively.

When $m = 4$, by Definition 2.7, the vertices of the Gauss-Lobatto polygons of $\mathbf{q}$ and $\mathbf{p}$ are

$$\mathbf{q}_0 = 0, \quad \mathbf{q}_1 = \frac{\mathbf{c}_1}{4}, \quad \mathbf{q}_2 = \frac{(1 + \sqrt{5})(\mathbf{c}_1 + \mathbf{c}_2)}{8} + \frac{3 - \sqrt{5}}{8},$$

$$\mathbf{q}_3 = \frac{3 + \mathbf{c}_2}{4}, \quad \mathbf{q}_4 = 1 \tag{3.9}$$

and

$$\mathbf{p}_0 = 0, \quad \mathbf{p}_1 = \frac{\mathbf{w}_0}{12},$$

$$\mathbf{p}_2 = \frac{1}{360}[(16\sqrt{5} + 30)\mathbf{w}_0^2 + (15 + 21\sqrt{5})\mathbf{w}_0\mathbf{w}_1 + (10 + 6\sqrt{5})\mathbf{w}_1^2 + (5 + 3\sqrt{5})\mathbf{w}_0\mathbf{w}_2 - (3\sqrt{5} - 15)\mathbf{w}_1\mathbf{w}_2 + 105 - 45\sqrt{5}],$$

$$\mathbf{p}_3 = \frac{1}{36}(3\mathbf{w}_0^2 + 2\mathbf{w}_1^2 + 3\mathbf{w}_1\mathbf{w}_2 + 3\mathbf{w}_0\mathbf{w}_1 + \mathbf{w}_0\mathbf{w}_2 + 21), \quad \mathbf{p}_4 = 1, \tag{3.10}$$

respectively. We identify the quintic PH curve $\mathbf{p}$ by minimizing the quantity

$$\Delta = |\mathbf{p}_1 - \mathbf{q}_1|^2 + |\mathbf{p}_2 - \mathbf{q}_2|^2 + |\mathbf{p}_3 - \mathbf{q}_3|^2 \tag{3.11}$$

with constraints (3.8). Substituting (3.9) and (3.10) into (3.11), simplifying, omitting terms that do not depend on $\mathbf{w}_0, \mathbf{w}_1, \mathbf{w}_2$, we obtain the following reduced form

$$\Delta = \frac{1}{1080}[18\bar{\mathbf{w}}_0^2[(24 + 6\sqrt{5})\mathbf{w}_0^2 + (18 + 5\sqrt{5})\mathbf{w}_0\mathbf{w}_1 + (4 + \sqrt{5})\mathbf{w}_0\mathbf{w}_2 + (8 + 2\sqrt{5})\mathbf{w}_1^2 +$$

$$(6 + \sqrt{5})\mathbf{w}_1\mathbf{w}_2] + 3\bar{\mathbf{w}}_0\bar{\mathbf{w}}_1[6(18 + 5\sqrt{5})\mathbf{w}_0^2 + 3(37 + 7\sqrt{5})\mathbf{w}_0\mathbf{w}_1 + (46 + 10\sqrt{5})\mathbf{w}_1^2 +$$

$$(23 + 5\sqrt{5})\mathbf{w}_0\mathbf{w}_2 + (27 + 9\sqrt{5})\mathbf{w}_1\mathbf{w}_2] + 3\bar{\mathbf{w}}_1\bar{\mathbf{w}}_2[(36 + 6\sqrt{5})\mathbf{w}_0^2 + (27 + 9\sqrt{5})\mathbf{w}_0\mathbf{w}_1 +$$

$$(22 + 2\sqrt{5})\mathbf{w}_1^2 + (11 + \sqrt{5})\mathbf{w}_0\mathbf{w}_2 + (39 - 3\sqrt{5})\mathbf{w}_1\mathbf{w}_2] + (2\bar{\mathbf{w}}_1^2 + \bar{\mathbf{w}}_0\bar{\mathbf{w}}_2)(18(4 + \sqrt{5})\mathbf{w}_0^2 +$$

$$(69 + 15\sqrt{5})\mathbf{w}_0\mathbf{w}_1 + (34 + 6\sqrt{5})\mathbf{w}_1^2 + (17 + 3\sqrt{5})\mathbf{w}_0\mathbf{w}_2 + (33 + 3\sqrt{5})\mathbf{w}_1\mathbf{w}_2)] +$$

$$2\mathrm{Re}(T_4 - T_5 - T_6), \tag{3.12}$$

where

$$T_4 = (\bar{\mathbf{q}}_1 + 18\sqrt{5} - 9)\mathbf{w}_0^2 + (51\sqrt{5} - 84)\mathbf{w}_0\mathbf{w}_1 + (4 + 6\sqrt{5})\mathbf{w}_1^2 + (3\sqrt{5} + 2)\mathbf{w}_0\mathbf{w}_2 +$$

$$(96 - 33\sqrt{5})\mathbf{w}_1\mathbf{w}_2,$$

$$T_5 = \frac{1}{30}\bar{\mathbf{q}}_2[(30 + 18\sqrt{5})\mathbf{w}_0^2 + (15 + 21\sqrt{5})\mathbf{w}_0\mathbf{w}_1 + (10 + 6\sqrt{5})\mathbf{w}_1^2 + (5 + 3\sqrt{5})\mathbf{w}_0\mathbf{w}_2 +$$

$$(15 - 3\sqrt{5})\mathbf{w}_1\mathbf{w}_2],$$

$$T_6 = \frac{1}{3}\bar{\mathbf{q}}_3(3\mathbf{w}_0^2 + 3\mathbf{w}_0\mathbf{w}_1 + 2\mathbf{w}_1^2 + \mathbf{w}_0\mathbf{w}_2 + 3\mathbf{w}_1 + \mathbf{w}_2).$$

By Lagrange multiplier method and Newton-Raphson iteration, this minimization problem with constraints can be solved.

The cases of $m = 5, 6, 7$ can be discussed similarly.

3.3. G^0 PH quintic closest to a cubic Bézier curve with prescribed arc length

It may be desirable to guarantee that the PH curve **p** matches not only the end points, but also the prescribed arc length L. In this section, we identify the PH quintic curve **p** which is G^0 closest to the cubic Bézier curve **q** and has a specified arc length L by Gauss-Lobatto and Gauss-Legendre polygon respectively.

For a planar quintic PH curve **p** with specified arc length L, the complex coefficients $\mathbf{w}_i$ in (3.2) must [14] satisfy the condition

$$2\left|\mathbf{w}_1\right|^2 + 3\mathrm{Re}((\bar{\mathbf{w}}_0 + \bar{\mathbf{w}}_2)\mathbf{w}_1) + 3\left|\mathbf{w}_0\right|^2 + 3\left|\mathbf{w}_2\right|^2 + \mathrm{Re}(\bar{\mathbf{w}}_0\mathbf{w}_2) = 15L,$$

which can be expressed as

$$s(u_0, v_0, u_1, v_1, u_2, v_2) = 0, \tag{3.13}$$

where

$$s = 2(u_1^2 + v_1^2) + 3(u_0u_1 + v_0v_1 + u_2u_1 + v_1v_2 + u_0^2 + v_0^2 + u_2^2 + v_2^2) + u_0u_2 + v_0v_2 - 15L.$$

To force the quintic PH curve **p** to have the same arc length L as a given ordinary cubic curve **q**, this condition must be introduced as a constraint with an associated Lagrange multiplier γ. The goal is to minimize the function $\Delta(u_0, v_0, u_1, v_1, u_2, v_2)$ as (3.7) and (3.12) corresponding to Gauss-Legendre and Gauss-Lobatto polygon respectively subject to the constraints (3.8) and (3.13). By the Lagrange multiplier method, the optimization problem then incurs a system of 9 equations in 9 real unknowns:

$$f_1 = \frac{\partial\Delta}{\partial u_0} + \alpha\frac{\partial g}{\partial u_0} + \beta\frac{\partial h}{\partial u_0} + \gamma\frac{\partial s}{\partial u_0} = 0, \quad f_2 = \frac{\partial\Delta}{\partial v_0} + \alpha\frac{\partial g}{\partial v_0} + \beta\frac{\partial h}{\partial v_0} + \gamma\frac{\partial s}{\partial v_0} = 0,$$

$$f_3 = \frac{\partial\Delta}{\partial u_1} + \alpha\frac{\partial g}{\partial u_1} + \beta\frac{\partial h}{\partial u_1} + \gamma\frac{\partial s}{\partial u_1} = 0, \quad f_4 = \frac{\partial\Delta}{\partial v_1} + \alpha\frac{\partial g}{\partial v_1} + \beta\frac{\partial h}{\partial v_1} + \gamma\frac{\partial s}{\partial v_1} = 0,$$

$$f_5 = \frac{\partial\Delta}{\partial u_2} + \alpha\frac{\partial g}{\partial u_2} + \beta\frac{\partial h}{\partial u_2} + \gamma\frac{\partial s}{\partial u_2} = 0, \quad f_6 = \frac{\partial\Delta}{\partial v_2} + \alpha\frac{\partial g}{\partial v_2} + \beta\frac{\partial h}{\partial v_2} + \gamma\frac{\partial s}{\partial v_2} = 0,$$

$$f_7 = g = 0, \quad f_8 = h = 0, \quad f_9 = s = 0.$$

Remark 3.1 The principles described in Sections 3.1–3.3 for determining the quintic PH curve closest to a given cubic Bézier curve (with prescribed arc length) can be readily generalized to quintic Bézier curves.

4. Computed examples

The following examples serve to illustrate the above algorithm in operation. The complicated nature of the objective functions $\Delta(u_0, v_0, u_1, v_1, u_2, v_2)$ and constraints (3.8) and (3.13) precludes a rigorous analysis of the number and nature of the extrema that the optimization problem admits. Consequently, in the following, this issue is investigated empirically for all the examples in [3] using the Newton-Raphson iterations. For the case without arc length constraint, choose the initial vector $\mathbf{x}_0$ of the unknown vector $\mathbf{x} = (u_0, v_0, u_1, v_1, u_2, v_2, \alpha, \beta)^{\mathrm{T}}$ as setting

$$\alpha = \beta = 1, \ \mathbf{w}_0 = u_0 + iv_0 = \sqrt{\lambda_0}\exp(i\frac{1}{2}\theta_0), \ \mathbf{w}_2 = u_2 + iv_2 = \sqrt{\lambda_1}\exp(i\frac{1}{2}\theta_1)$$

with $\mathbf{w}_1$ the complex root of (3.3) that yields the smaller value of $\triangle$, where λ_0, λ_1 and θ_0, θ_1 are the magnitudes and arguments of the end derivatives $\mathbf{q}'(0)$ and $\mathbf{q}'(1)$; for the case with arc length constraint, choose the initial value $\alpha = \beta = \gamma = 1$ together with $\mathbf{w}_0 = \lambda_0 \exp(i\frac{1}{2}\theta_0)$ and $\mathbf{w}_1, \mathbf{w}_2$ the complex root of (3.3) and (3.13) that yields the smaller value of $\triangle$. The choice of $\mathbf{w}_0, \mathbf{w}_1$ and $\mathbf{w}_2$ values defines end derivatives identical to those of the curve being approximated, and ensures satisfaction of the end-point condition. To check if the convergence efficiency and consistency depends on the choice $(\alpha, \beta) = (1, 1)$, the examples below were repeated with $(\alpha, \beta) = (0, 0)$ and $(-1, -1)$. In all of these cases, the same converged solution was obtained, with a number of iterations differing by no more than one. The iterations stop when $\|\delta\mathbf{x}_k\| \leq 10^{-15}$.

(a) Ld ($m = 3$)	(b) Ld ($m = 4$)	(c) Ld ($m = 5$)	(d) Lb ($m = 4$)
(e) Lb ($m = 5$)	(f) Lb ($m=6$)	(g) Lb ($m = 7$)	(h) G^0 method in [3]
(i) Ld$_-$Arc ($m = 3$)	(j) Ld$_-$Arc ($m = 4$)	(k) Lb$_-$Arc ($m = 5$)	(l) Lb$_-$Arc ($m = 4$)
(m) Lb$_-$Arc ($m = 5$)	(n) Lb$_-$Arc ($m = 6$)	(o) Lb$_-$Arc ($m = 7$)	
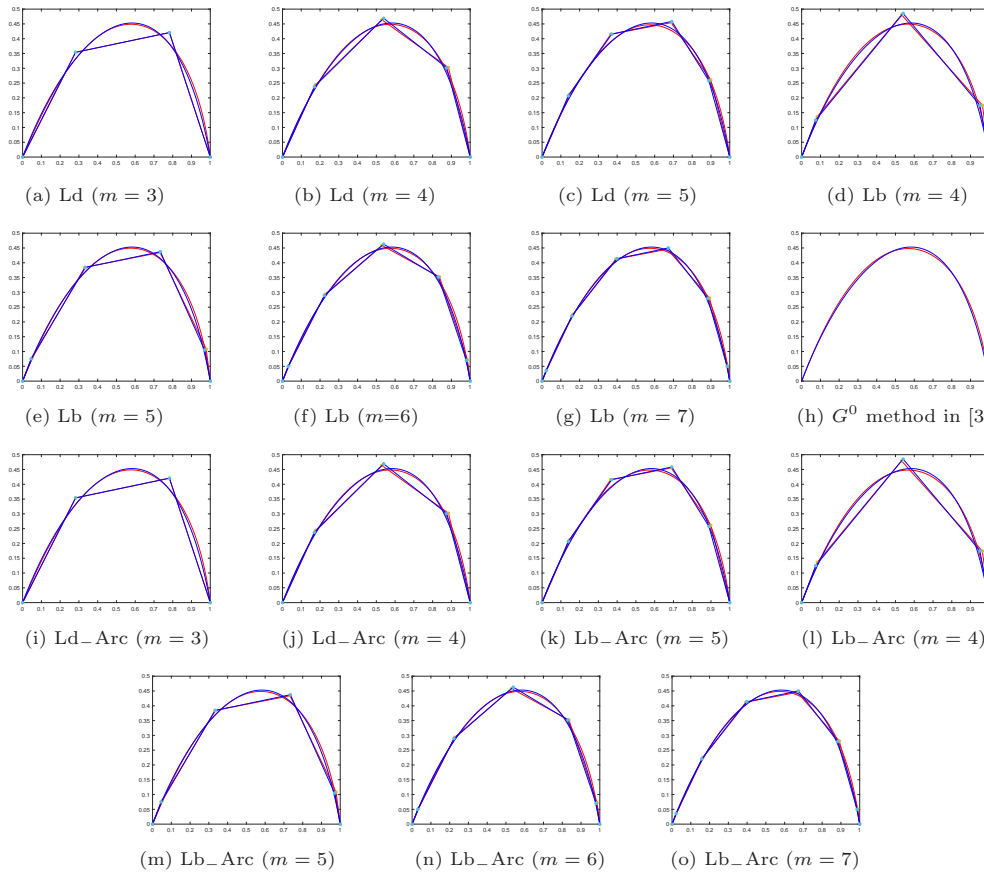
Figure 1 The quintic PH curve $\mathbf{p}$ (red curves and red control polygons) closest to $\mathbf{q}$ (blue curves and blue control polygons) in Example 4.1

To assess the closeness of the PH quintic $\mathbf{p}$ with a prescribed cubic or quintic Bézier curve $\mathbf{q}$, several measures are used:

$$e_0 = \Big(\frac{1}{6}\sum_{k=0}^{5}|\mathbf{b}_k - \mathbf{d}_k|\Big)^{\frac{1}{2}}, \quad e_1 = \Big(\frac{1}{m}\sum_{k=0}^{m-1}|\mathbf{p}_k - \mathbf{q}_k|\Big)^{\frac{1}{2}},$$

$$e_2 = \Big(\int_0^1 |\mathbf{p}(t) - \mathbf{q}(t)|^2 \mathrm{d}t\Big)^{\frac{1}{2}}, \quad e_3 = |L - l|,$$

where $\{\mathbf{d}_k\}$ are the Bézier control points of $\mathbf{q}$ after degree elevation and L, l denote the arc lengths of the curves $\mathbf{p}$ and $\mathbf{q}$, respectively.

Number of nodes	Δ	e_0	e_1	e_2	e_3	Number of iterations
Ld ($m=3$)	0	2.65×10^{-2}	0	6.39×10^{-3}	3.62×10^{-4}	5
Ld ($m=4$)	2.80×10^{-4}	2.46×10^{-2}	7.48×10^{-3}	6.05×10^{-3}	4.12×10^{-4}	5
Ld ($m=5$)	2.31×10^{-4}	2.52×10^{-2}	6.21×10^{-3}	7.05×10^{-3}	2.24×10^{-3}	5
Lb ($m=4$)	4.57×10^{-4}	2.37×10^{-2}	9.56×10^{-3}	7.66×10^{-3}	2.50×10^{-3}	5
Lb ($m=5$)	1.48×10^{-4}	2.53×10^{-2}	4.97×10^{-3}	5.91×10^{-3}	1.50×10^{-3}	5
Lb ($m=6$)	2.17×10^{-4}	2.50×10^{-2}	5.56×10^{-3}	5.94×10^{-3}	9.07×10^{-4}	5
Lb ($m=7$)	2.41×10^{-4}	2.50×10^{-2}	5.50×10^{-3}	5.95×10^{-3}	7.83×10^{-4}	5
G^0 method in [3]	3.32×10^{-3}	2.35×10^{-2}		7.43×10^{-3}	1.05×10^{-3}	5
Ld_Arc ($m=3$)	6.96×10^{-8}	2.65×10^{-2}	1.32×10^{-4}	6.40×10^{-3}	0	5
Ld_Arc ($m=4$)	2.80×10^{-4}	2.46×10^{-2}	7.48×10^{-3}	6.07×10^{-3}	0	5
Ld_Arc ($m=5$)	2.34×10^{-4}	2.53×10^{-2}	6.25×10^{-3}	6.86×10^{-3}	0	5
Lb_Arc ($m=4$)	4.60×10^{-4}	2.37×10^{-2}	9.59×10^{-3}	7.66×10^{-3}	0	5
Lb_Arc ($m=5$)	1.49×10^{-4}	2.53×10^{-2}	4.99×10^{-3}	5.95×10^{-3}	0	5
Lb_Arc ($m=6$)	2.17×10^{-4}	2.50×10^{-2}	5.57×10^{-3}	5.97×10^{-3}	0	5
Lb_Arc ($m=7$)	2.42×10^{-4}	2.51×10^{-2}	5.50×10^{-3}	5.98×10^{-3}	0	5

Table 3   The errors of quintic PH curves closest to $\mathbf{q}$ in Example 4.1

4.1. Quintic PH curve closest to a cubic Bézier curve

Number of nodes	Δ	e_0	e_1	e_2	e_3	Number of iterations
Ld ($m=3$)	0	7.92×10^{-2}	0	1.05×10^{-2}	6.01×10^{-3}	6
Ld ($m=4$)	6.59×10^{-5}	7.75×10^{-2}	3.63×10^{-3}	6.33×10^{-3}	4.59×10^{-3}	5
Ld ($m=5$)	3.38×10^{-4}	7.65×10^{-2}	7.50×10^{-3}	7.70×10^{-3}	2.70×10^{-3}	6
Lb ($m=4$)	1.09×10^{-4}	7.69×10^{-2}	4.66×10^{-3}	1.62×10^{-2}	5.77×10^{-3}	5
Lb ($m=5$)	5.41×10^{-4}	7.49×10^{-2}	9.49×10^{-3}	6.47×10^{-3}	1.38×10^{-3}	5
Lb ($m=6$)	1.93×10^{-4}	7.70×10^{-3}	5.25×10^{-3}	5.87×10^{-3}	4.98×10^{-3}	5
Lb ($m=7$)	2.76×10^{-4}	7.67×10^{-3}	5.87×10^{-3}	5.91×10^{-3}	4.04×10^{-3}	5
G^0 method in [3]	2.34×10^{-2}	6.24×10^{-2}		1.95×10^{-2}	4.82×10^{-2}	5
Ld_Arc ($m=3$)	4.98×10^{-5}	7.47×10^{-2}	3.53×10^{-3}	1.06×10^{-2}	0	5
Ld_Arc ($m=4$)	7.57×10^{-5}	7.56×10^{-2}	3.89×10^{-3}	6.55×10^{-3}	0	5
Ld_Arc ($m=5$)	3.42×10^{-4}	7.53×10^{-2}	7.55×10^{-3}	7.73×10^{-3}	0	6
Lb_Arc ($m=4$)	2.31×10^{-4}	8.30×10^{-2}	6.80×10^{-3}	1.46×10^{-2}	0	5
Lb_Arc ($m=5$)	5.42×10^{-4}	7.43×10^{-2}	9.50×10^{-3}	6.56×10^{-3}	0	5
Lb_Arc ($m=6$)	2.05×10^{-4}	7.49×10^{-2}	5.42×10^{-3}	6.11×10^{-3}	0	5
Lb_Arc ($m=7$)	2.85×10^{-4}	7.50×10^{-2}	5.97×10^{-3}	6.14×10^{-3}	0	6

Table 4   The errors of quintic PH curves closest to $\mathbf{q}$ in Example 4.2

The following examples illustrate application of the method to cubic Bézier curves.

Example 4.1   Consider the C-shaped canonical-form cubic Bézier curve $\mathbf{q}$ defined by the control points

$$\mathbf{c}_0 = 0,\ \mathbf{c}_1 = 0.3 + 0.5i,\ \mathbf{c}_2 = 0.8 + 0.7i,\ \mathbf{c}_3 = 1.$$

Its arc length is $l = 1.4304$. Figure 1 compares the G^0 PH quintics **p** closest to **q** obtained by Gauss-Lobatto polygon, Gauss-Legendre polygon and the method in [3] respectively, where Ld_Arc and Ld denote the G^0 quintic PH curves obtained by Gauss-Legendre polygon with and without prescribed arc length respectively, while Lb_Arc and Lb denote the G^0 quintic PH curves obtained by Gauss-Lobatto polygon with and without prescribed arc length respectively. Table 3 illustrates various errors between the quintic PH curves **p** and cubic Bézier curve **q**. As evident from the results, in cases where the arc length is not specified, all the approximations are seen to closely approximate the given cubic curve, while Ld with $m = 3, 4$ and Lb with $m = 6, 7$ conform somewhat more closely since they have closer arc length. In cases where the arc length $L = l$ is specified, all the Ld_Arc and Lb_Arc approximate the original curve **q** very well.

(a) Ld $(m = 3)$ (b) Ld $(m = 4)$ (c) Ld $(m = 5)$ (d) Lb $(m = 4)$

(e) Lb $(m = 5)$ (f) Lb $(m=6)$ (g) Lb $(m = 7)$ (h) G^0 method in [3]

(i) Ld _Arc $(m = 3)$ (j) Ld_Arc $(m = 4)$ (k) Lb_Arc $(m = 5)$ (l) Lb_Arc $(m = 4)$

(m) Lb_Arc $(m = 5)$ (n) Lb_Arc $(m = 6)$ (o) Lb_Arc $(m = 7)$
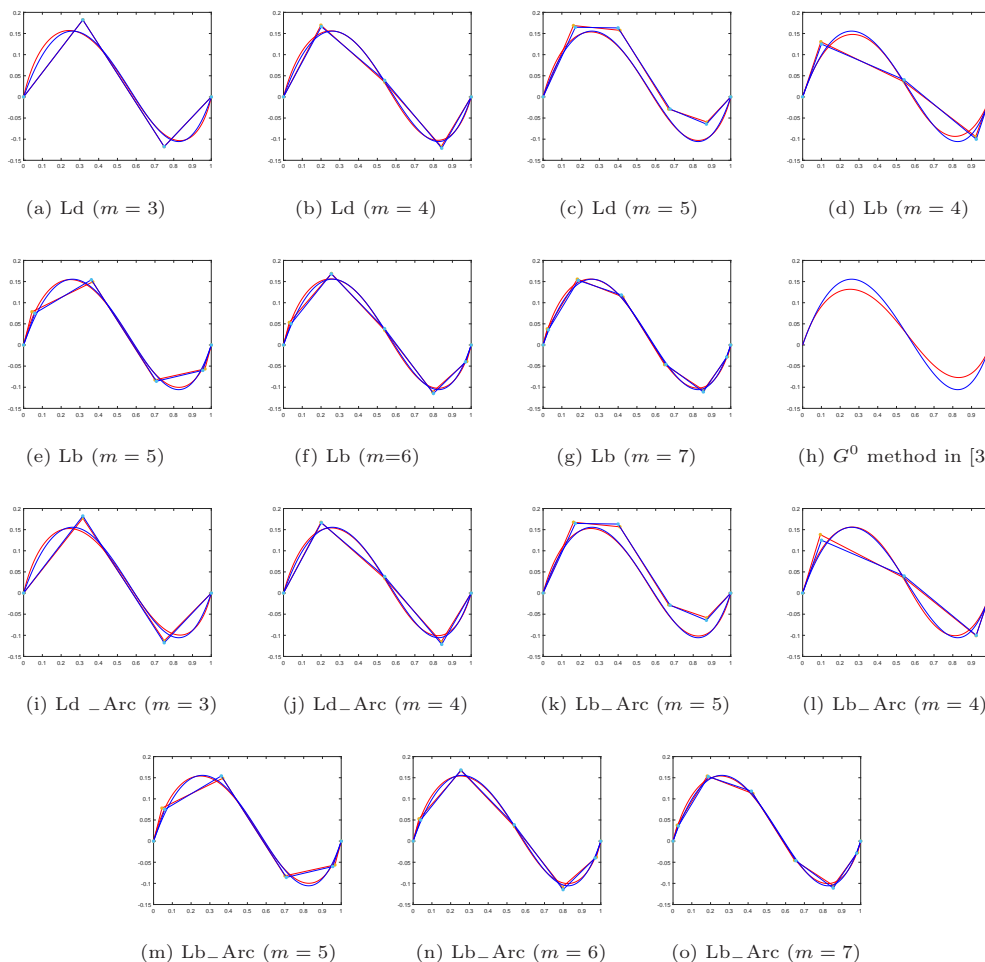
Figure 2 The quintic PH curves **p** closest to a cubic Bézier curve **q** in Example 4.2

This example demonstrates that for convex cubic segments, the Gauss-Lobatto and Gauss-Legendre polygon can achieve the same good results with Bézier control polygon when without arc length constraint, and since the edge number m has more choices, even better results can

be achieved; when the arc length is constrained, both the arc length preserving and good approximate effect can be achieved. It should be noted that the Ld with $m = 3$ has the same Gauss-Legendre polygon with $\mathbf{q}$. This is coincident with Theorem 2.5.

Example 4.2 Consider the S-shaped canonical-form cubic Bézier curve $\mathbf{q}$ defined by the control points

$$\mathbf{c}_0 = 0, \ \mathbf{c}_1 = 0.4 + 0.5i, \ \mathbf{c}_2 = 0.7 - 0.4i, \ \mathbf{c}_3 = 1$$

with the arc length $l = 1.1586$. Figure 2 compares the PH quintic $\mathbf{p}$ closest to the cubic Bézier curve $\mathbf{q}$ obtained by Gauss-Lobatto polygon and Gauss-Legendre polygon with and without arc length constraint. Table 4 illustrates various errors between $\mathbf{p}$ and $\mathbf{q}$. Because of the stronger curvature variation of the cubic curve $\mathbf{q}$, the G^0 PH quintic obtained by Bézier control polygon in [3] is not close to the original curve, while our method works very well with small error and close arc length. Moreover, even with specified arc length $L = l$, the approximation effect of the curves $\mathbf{p}$ is still very good.

(a) Ld ($m = 3$) (b) Ld ($m = 4$) (c) Ld ($m = 5$) (d) Lb ($m = 4$)

(e) Lb ($m = 5$) (f) Lb ($m=6$) (g) Lb ($m = 7$) (h) G^0 method in [3]

(i) Ld $_-$Arc ($m = 3$) (j) Ld$_-$Arc ($m = 4$) (k) Lb$_-$Arc ($m = 5$) (l) Lb$_-$Arc ($m = 4$)

(m) Lb$_-$Arc ($m = 5$) (n) Lb$_-$Arc ($m = 6$) (o) Lb$_-$Arc ($m = 7$)
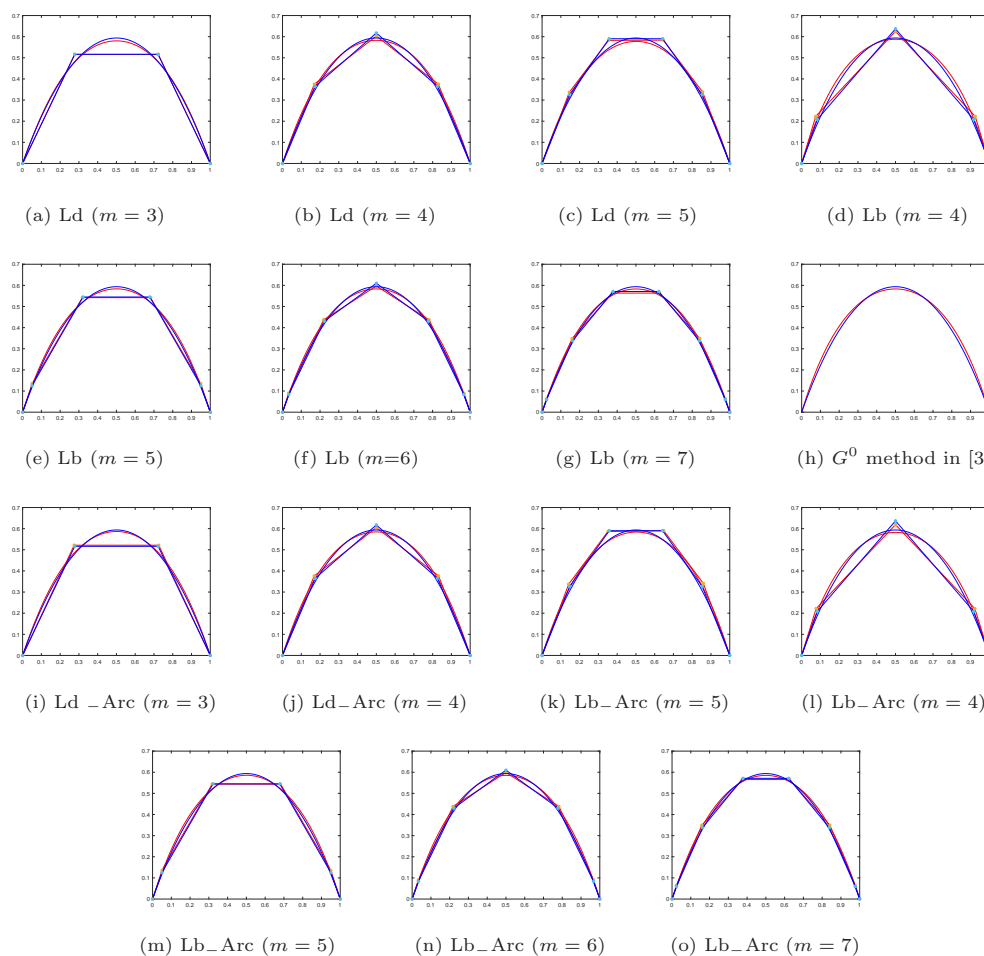
Figure 3 The quintic PH curves $\mathbf{p}$ closest to a quintic Bézier curve $\mathbf{q}$ in Example 4.3

This example demonstrates that for inflectional segments, the method by Gauss-Lobatto and Gauss-Legendre polygon can achieve good approximation results.

Examples 4.1 and 4.2 highlight that the closest PH quintics offer good G^0 approximants for both convex and inflectional cubic segments.

4.2. Quintic PH curve closest to a quintic Bézier curve

The following examples illustrate applications of the method to quintic Bézier curves. Note that quintic Bézier curves have twice as many free shape parameters as quintic PH curves, so the quintic PH curve closest to a given quintic Bézier curve may not always be a reasonable approximation.

Example 4.3 Consider the C-shaped canonical-form quintic Bézier curve $\mathbf{q}$ defined by the control points

$$\bar{\mathbf{c}}_0 = 0, \ \bar{\mathbf{c}}_1 = 0.2 + 0.5i, \ \bar{\mathbf{c}}_2 = 0.4 + 0.7i, \ \bar{\mathbf{c}}_3 = 0.6 + 0.7i, \ \bar{\mathbf{c}}_4 = 0.8 + 0.5i, \ \bar{\mathbf{c}}_5 = 1.$$

Its arc length is $l = 1.6298$. Figure 3 compares the PH quintics $\mathbf{p}$ closest to $\mathbf{q}$ obtained by Gauss-Lobatto polygon, Gauss-Legendre polygon and the method in [3], respectively. Table 5 illustrates various errors between the quintic PH curves $\mathbf{p}$ and quintic Bézier curve $\mathbf{q}$.

The results demonstrate that comparied with the method in [3], the Ld with $m = 4$ and Lb with $m \geq 5$ are better approximants to the given curve $\mathbf{q}$ with smaller error and similar arc length. Moreover, the Ld_Arc with $m = 3, 4$ and Lb_Arc with $m \geq 5$ can achieve good approximation effect with prescribed arc length $L = l$.

Number of nodes	Δ	e_0	e_1	e_2	e_3	Number of iterations
Ld $(m = 3)$	0	3.82×10^{-2}	0	8.84×10^{-3}	1.26×10^{-2}	5
Ld $(m = 4)$	4.71×10^{-4}	3.36×10^{-2}	9.70×10^{-3}	8.06×10^{-3}	3.50×10^{-3}	5
Ld $(m = 5)$	4.01×10^{-4}	3.44×10^{-2}	8.17×10^{-3}	9.39×10^{-3}	1.30×10^{-2}	5
Lb $(m = 4)$	7.01×10^{-4}	3.20×10^{-2}	1.18×10^{-2}	1.08×10^{-2}	1.04×10^{-2}	5
Lb $(m = 5)$	2.71×10^{-4}	3.51×10^{-2}	6.72×10^{-3}	7.81×10^{-3}	3.98×10^{-3}	5
Lb $(m = 6)$	3.75×10^{-4}	3.44×10^{-2}	7.32×10^{-3}	7.86×10^{-3}	3.96×10^{-3}	5
Lb $(m = 7)$	4.18×10^{-4}	3.44×10^{-2}	7.23×10^{-3}	7.87×10^{-3}	4.19×10^{-3}	5
G^0 method in [3]	6.04×10^{-3}	3.17×10^{-2}		1.05×10^{-2}	2.16×10^{-3}	5
Ld_Arc $(m = 3)$	7.52×10^{-5}	3.64×10^{-2}	4.33×10^{-3}	8.19×10^{-3}	0	5
Ld_Arc $(m = 4)$	4.77×10^{-4}	3.33×10^{-2}	9.77×10^{-3}	8.07×10^{-3}	0	5
Ld_Arc $(m = 5)$	5.07×10^{-4}	3.27×10^{-2}	9.19×10^{-3}	8.70×10^{-3}	0	5
Lb_Arc $(m = 4)$	7.47×10^{-4}	3.18×10^{-2}	1.22×10^{-2}	1.01×10^{-2}	0	5
Lb_Arc $(m = 5)$	2.79×10^{-4}	3.46×10^{-2}	6.82×10^{-3}	7.87×10^{-3}	0	5
Lb_Arc $(m = 6)$	3.85×10^{-4}	3.40×10^{-2}	7.41×10^{-3}	7.90×10^{-3}	0	5
Lb_Arc $(m = 7)$	4.31×10^{-4}	3.39×10^{-2}	7.34×10^{-3}	7.90×10^{-3}	0	5

Table 5 The errors of quintic PH curves closest to $\mathbf{q}$ in Example 4.3

(a) Ld ($m = 3$)   (b) Ld ($m = 4$)   (c) Ld ($m = 5$)   (d) Lb ($m = 4$)

(e) Lb ($m = 5$)   (f) Lb ($m=6$)   (g) Lb ($m = 7$)   (h) G^0 method in [3]

(i) Ld$_-$Arc ($m = 3$)   (j) Ld$_-$Arc ($m = 4$)   (k) Lb$_-$Arc ($m = 5$)   (l) Lb$_-$Arc ($m = 4$)

(m) Lb$_-$Arc ($m = 5$)   (n) Lb$_-$Arc ($m = 6$)   (o) Lb$_-$Arc ($m = 7$)
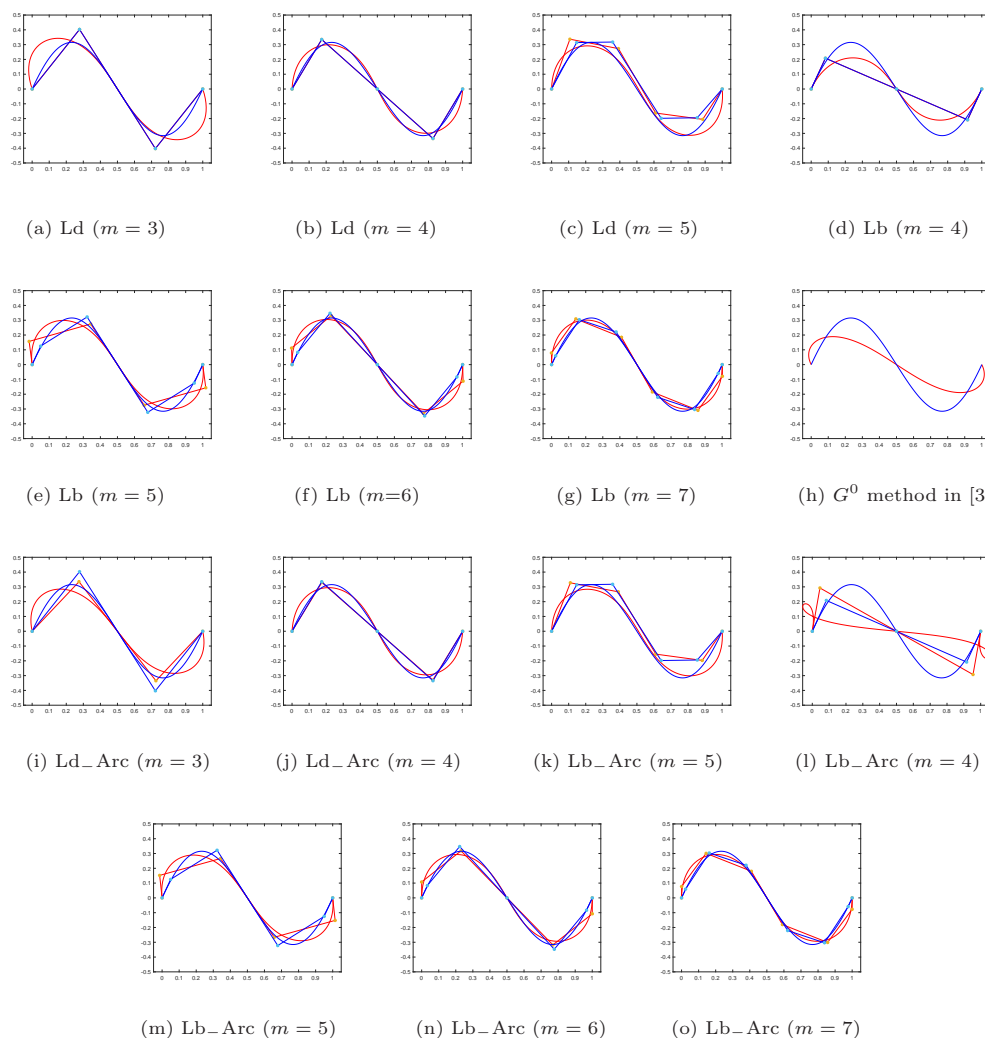
Figure 4 The quintic PH curves $\mathbf{p}$ closest to a quintic Bézier curve $\mathbf{q}$ in Example 4.4

Example 4.4 Consider the S-shaped canonical-form quintic Bézier curve $\mathbf{q}$ defined by the control points

$$\bar{\mathbf{c}}_0 = 0, \ \bar{\mathbf{c}}_1 = 0.2 + 0.5i, \ \bar{\mathbf{c}}_2 = 0.4 + 0.7i, \ \bar{\mathbf{c}}_3 = 0.6 - 0.7i, \ \bar{\mathbf{c}}_4 = 0.8 - 0.5i, \ \bar{\mathbf{c}}_5 = 1$$

with the arc length $l = 1.6732$. Figure 4 compares the PH quintics $\mathbf{p}$ closest to $\mathbf{q}$ obtained by Gauss-Lobatto polygon, Gauss-Legendre polygon and the method in [3] respectively. Table 6 illustrates various errors between the quintic PH curves $\mathbf{p}$ and quintic Bézier curve $\mathbf{q}$. For this inflectional quintic curve $\mathbf{q}$ with a strong curvature variation, the results demonstrate that comparied with the G^0 method in [3], the Ld with $m \geq 4$ and Lb with $m \geq 5$ are closer to the given curve $\mathbf{q}$ with smaller error and closer arc length, while all the Ld$_-$Arc and Lb$_-$Arc with $m \geq 5$ are better approximants with the arc length constraint $L = l$.

Number of nodes	Δ	e_0	e_1	e_2	e_3	Number of iterations
Ld $(m=3)$	0	4.62×10^{-1}	0	5.97×10^{-2}	2.25×10^{-1}	8
Ld $(m=4)$	0	4.48×10^{-1}	0	3.29×10^{-2}	1.59×10^{-2}	6
Ld $(m=5)$	8.65×10^{-3}	4.34×10^{-1}	3.80×10^{-2}	3.65×10^{-2}	3.63×10^{-2}	7
Lb $(m=4)$	0	4.12×10^{-1}	0	8.57×10^{-2}	2.93×10^{-1}	7
Lb $(m=5)$	1.66×10^{-2}	4.10×10^{-1}	5.27×10^{-2}	3.56×10^{-2}	3.45×10^{-2}	7
Lb $(m=6)$	4.87×10^{-3}	4.41×10^{-1}	2.64×10^{-2}	3.00×10^{-2}	4.32×10^{-2}	7
Lb $(m=7)$	7.43×10^{-3}	4.36×10^{-1}	3.05×10^{-2}	3.03×10^{-2}	2.81×10^{-2}	7
G^0 method in [3]	4.89×10^{-1}	2.86×10^{-1}		1.21×10^{-1}	2.66×10^{-1}	8
Ld_Arc $(m=3)$	9.27×10^{-3}	3.77×10^{-1}	4.81×10^{-2}	4.86×10^{-2}	0	6
Ld_Arc $(m=4)$	4.81×10^{-5}	4.43×10^{-1}	3.10×10^{-3}	3.37×10^{-2}	0	7
Ld_Arc $(m=5)$	8.92×10^{-3}	4.22×10^{-1}	3.86×10^{-2}	3.67×10^{-2}	0	7
Lb_Arc $(m=4)$	1.70×10^{-2}	1.20	5.84×10^{-2}	2.34×10^{-1}	0	7
Lb_Arc $(m=5)$	1.69×10^{-2}	3.99×10^{-1}	5.30×10^{-2}	3.67×10^{-2}	0	6
Lb_Arc $(m=6)$	5.24×10^{-3}	4.26×10^{-1}	2.74×10^{-2}	3.16×10^{-2}	0	7
Lb_Arc $(m=7)$	7.61×10^{-3}	4.27×10^{-1}	3.08×10^{-2}	3.17×10^{-2}	0	7

Table 6 The errors of quintic PH curves closest to **q** in Example 4.4

Examples 4.3 and 4.4 highlight that the closest PH quintics offer better approximants to convex quintic segments than to inflectional segments.

Example 4.5 In this final example, a quintic PH curve is modified by perturbing a single control point so that the perturbed curve is no longer a PH curve, as shown in Figure 5(a). We then determine the G^0 quintic PH curve closest to the modified curve by Gauss-Legendre and Gauss-Lobatto polygon respectively. Figure 5 compares the Ld and Lb with different edge number m and the one by the method in [3]. Table 7 illustrates various errors between the quintic PH curves **p** and quintic Bézier curve **q**.

The result demonstrates that for this case, our method with Gauss-Legendre and Gauss-Lobatto polygon can still obtain better approximation with smaller error and closer arc length than the method by Bézier control polygon.

Remark 4.6 The problems are investigated empirically for Examples 4.1–4.5 by starting the Newton-Raphson iterations from points satisfying the constraints and yielding smaller objective functions. It was found that when the procedure converges in a reasonable number of iterations, the resulting values correspond to a unique solution. Moreover, as evident from Tables 3–7 for all the examples, the initial values of the optimization variables proposed in our method yield rapid convergence (with between 5 and 8 iterations) to the unique solution.

It is noteworthy that [3] emphasized that the Bézier control polygon tends to exaggerate the behavior of the curve, so $e_0 > e_2$. However, in all the above examples, $e_1 > e_2$ does not always hold, which means that both the Gauss-Legendre and Gauss-Lobatto polygon do not exaggerate the shape of the curve. Moreover, the approximate effect of the PH quintic curve does not get better as the edge number m of Gauss-Legendre or Gauss-Lobatto polygon increases.

(a) a quintic PH curve
modified by displacement
of a single control point

(b) Ld ($m = 3$)

(c) Ld ($m = 4$)

(d) Ld ($m = 5$)

(e) Lb ($m = 5$)

(f) Lb ($m=6$)

(g) Lb ($m = 7$)

(h) G^0 method in [3]
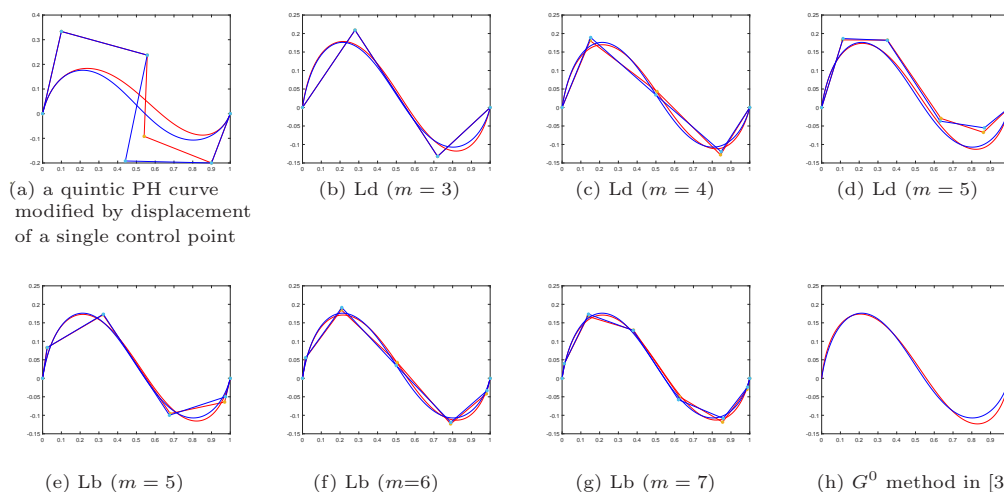
Figure 5   A quintic PH curve (red) modified by displacement of a single control point (blue) in (a); the
PH quintics closest to the modified curve in Example 4.5

Number of nodes	Δ	e_0	e_1	e_2	e_3	Number of iterations
Ld ($m = 3$)	0	4.72×10^{-2}	0	8.01×10^{-3}	1.60×10^{-2}	5
Ld ($m = 4$)	2.87×10^{-4}	4.70×10^{-2}	7.58×10^{-3}	6.62×10^{-3}	2.60×10^{-3}	5
Ld ($m = 5$)	2.70×10^{-4}	4.64×10^{-2}	6.71×10^{-3}	6.81×10^{-3}	3.82×10^{-3}	5
Lb ($m = 4$)	5.50×10^{-4}	4.76×10^{-2}	1.05×10^{-2}	1.05×10^{-2}	1.71×10^{-2}	5
Lb ($m = 5$)	2.76×10^{-4}	4.53×10^{-2}	6.78×10^{-3}	6.60×10^{-3}	6.63×10^{-3}	5
Lb ($m = 6$)	2.54×10^{-4}	4.66×10^{-2}	6.02×10^{-3}	6.46×10^{-3}	1.05×10^{-3}	5
Lb ($m = 7$)	3.00×10^{-4}	4.64×10^{-2}	6.12×10^{-3}	6.47×10^{-3}	6.91×10^{-3}	5
G^0 method in [3]	8.73×10^{-3}	3.82×10^{-2}		1.39×10^{-2}	2.18×10^{-2}	6

Table 7   The errors of quintic PH curves closest to $\mathbf{q}$ in Example 4.5

5. Conclusion

Bézier control polygon is not appropriate to control a Pythagorean-hodograph curve since
it has redundant degrees of freedom, so the Gauss-Legendre and Gauss-Lobatto polygon are
used instead in this context to construct PH curves. These two kinds of polygons for a planar
polynomial curve both have the end point interpolation property and their lengths can be viewed
as the approximations of the arc length of the polynomial curve. Therefore, the Gauss-Legendre
and Gauss-Lobatto polygon can be used to develop simple PH curve manipulation algorithms.

By expressing the sum of squared differences between the vertices of the Gauss-Legendre or
Gauss-Lobatto polygon of a given planar Bézier curve and those of a quintic PH curve in terms
of the complex coefficients, the task of identifying the PH curve with or without prescribed arc
length that is G^0 closest to the Bézier curve can be formulated as a constrained polynomial
optimization problem. By Lagrange multiplier method and the Newton-Raphson iterations,

examples of the approximation of cubic and quintic Bézier curves by quintic PH curves are presented. Better approximations can be achieved for flat curves or curves with severe curvature variation than that with Bézier control polygon. Moreover, the methodology can be readily adapted to higher degree PH curves.

References

[1] R. T. FAROUKI, T. SAKKALIS. *Pythagorean hodographs*. IBM Journal of Research and Development, 1990, **34**(5): 736–752.

[2] R. T. FAROUKI. *Pythagorean-Hodograph Curves*. Algebra and Geometry Inseparable, Springer, 2007.

[3] R. T. FAROUKI. *Identifying Pythagorean-hodograph curves closest to prescribed planar Bézier curves*. Comput.-Aided Des., 2022, **149**: Paper No. 103266, 9 pp.

[4] R. T. FAROUKI, C. GIANNELLI, A. SESTINI. *Identification and "reverse engineering" of Pythagorean-hodograph curves*. Comput. Aided Geom. Design, 2015, **34**: 21–36.

[5] R. T. FAROUKI, C. GIANNELLI, A. SESTINI. *Local modification of Pythagorean-hodograph quintic spline curves using the B-spline form*. Adv. Comput. Math., 2016, **42**(1): 199–225.

[6] S. H. KIM, H. P. MOON. *Rectifying control polygon for planar Pythagorean-hodograph curves*. Comput. Aided Geom. Design, 2017, **54**: 1–14.

[7] S. H. KIM, H. P. MOON. *Deformation of spatial septic Pythagorean-hodograph curves using Gauss-Legendre polygon*. Comput. Aided Geom. Design, 2019, **73**: 16–34.

[8] S. H. KIM, H. P. MOON. *Gauss-Lobatto polygon of Pythagorean-hodograph curves*. Comput. Aided Geom. Design, 2019, **74**: 101768, 20 pp.

[9] R. T. FAROUKI. *The conformal map $z \to z^2$ of the hodograph plane*. Comput. Aided Geom. Design, 1994, **11**(4): 36—390.

[10] P. DAVIS, P. RABINOWITZ. *Methods of Numerical Integration*. Second edition, Academic Press, New York, 1984.

[11] J. STOER, R. BULIRSCH. *Introduction to Numerical Analysis*. Second edition, Springer Verlag, New York, 1993.

[12] M. R. ESLAHCHI, M. M. JAMEI, E. BABOLIAN. *On numerical improvement of Gauss-Lobatto quadrature rules*. Appl. Math. Comput., 2005, **164**(3): 707–717.

[13] E. BABOLIAN, M. M. JAMEI, M. R. ESLAHCHI. *On numerical improvement of Gauss-Legendre quadrature rules*. Appl. Math. Comput., 2005, **160**(3): 779–789.

[14] R. T. FAROUKI. *Construction of G^1 planar Hermite interpolants with prescribed arc lengths*. Comput. Aided Geom. Design, 2016, **46**: 64–75.